ESRF	**Experiment title:** Force-correlated in situ attachment and retraction of adhesive spider hairs investigated with scanning nanodiffraction	**Experiment number**: SC-4299
Beamline: ID13	**Date of experiment**: from: 22. 06. 2016 to: 26. 06. 2016	**Date of report**:
Shifts: 12	**Local contact(s)**: Martin Rosenthal	*Received at ESRF:*

Names and affiliations of applicants (* indicates experimentalists):

***Schaber, Clemens**; Functional Morphology and Biomechanics, Zoological Institute, Kiel University, Am Botanischen Garten 9, 24118 Kiel, Germany

***Flenner, Silja;** Helmholtz-Zentrum Geesthacht, Max-Planck-Str. 1, 21502 Geesthacht, Germany and Institute of Experimental and Applied Physics, Kiel University, Leibnizstr. 19, 24118 Kiel, Germany

***Krasnov, Igor;** Institute of Experimental and Applied Physics, Kiel University, Leibnizstr. 19, 24118 Kiel, Germany

*Stieglitz, Hergen**;** Helmholtz-Zentrum Geesthacht, Max-Planck-Str. 1, 21502 Geesthacht, Germany and Institute of Experimental and Applied Physics, Kiel University, Leibnizstr. 19, 24118 Kiel, Germany

Gorb, Stanislav; Functional Morphology and Biomechanics, Zoological Institute, Kiel University, Am Botanischen Garten 9, 24118 Kiel, Germany

***Müller, Martin;** Helmholtz-Zentrum Geesthacht, Max-Planck-Str. 1, 21502 Geesthacht, Germany and Institute of Experimental and Applied Physics, Kiel University, Leibnizstr. 19, 24118 Kiel, Germany

Report:

Published paper

Hierarchical architecture of spider attachment setae reconstructed from scanning nanofocus X-ray diffraction data

Abstract

When sitting and walking, the feet of wandering spiders reversibly attach to many surfaces without the use of gluey secretions. Responsible for the spiders' dry adhesion are the hairy attachment pads that are built of specially shaped cuticular hairs (setae) equipped with approximately 1 mm wide and 20 nm thick plate-like contact elements (spatulae) facing the substrate. Using synchrotron-based scanning nanofocus X-ray diffraction methods, combining wide-angle X-ray diffraction/scattering and small-angle X-ray scattering, allowed substantial quantitative information to be gained about the structure and materials of these fibrous adhesive structures with 200 nm resolution. The fibre diffraction patterns showed the crystalline chitin chains oriented along the long axis of the attachment setae and increased intensity of the chitin signal dorsally within the seta shaft. The small-angle scattering signals clearly indicated an angular shift by approximately 808 of the microtrich structures that branch off the bulk hair shaft and end as the adhesive contact elements in the tip region of the seta. The results reveal the specific structural arrangement and distribution of the chitin fibres within the

attachment hair’s cuticle preventing material failure by tensile reinforcement and proper distribution of stresses that arise upon attachment and detachment.

Reference

Schaber CF, Flenner F, Glisovic A, Krasnov I, Rosenthal M, Stieglitz H, Krywka C, Burghammer M, Müller M, Gorb SN, 2019. Hierarchical architecture of spider attachment setae reconstructed from scanning nanofocus X-ray diffraction data. J. R. Soc. Interface 16: 20180692. DOI:10.1098/rsif2018.0692.

Paper to be submitted

Mechanical gradients of hierarchically structured spider attachment hairs

Abstract

Wandering spiders climb vertically and walk upside-down on rough and smooth surfaces using a nano-structured attachment system on their feet[1–3]. Similar to the gecko[4], the spiders are assumed to adhere by intermolecular van der Waals forces between the adhesive structures and the substrate. The adhesive elements are arranged highly-ordered on the hierarchically structured attachment hairs (setae) that are densely packed at the tips of the spiders’ feet. While walking, it is suggested that the spiders apply a shear force on their legs to increase friction by enlargement of the contact area[5–7]. However, it is not completely understood how the specialized structural features of the attachment hairs behave during attachment and detachment of the setae. Here, we show gradients of the mechanical properties of the attachment hairs on different length scales, evolved to support attachment, stabilize adhesion in contact, and withstand high stress at detachment. We demonstrate how the approximately 20 nm thin spatulae, the adhesive elements at the tips of the setal branches, make contact to the surface. Shearing of the hairs helps the adhesive elements to self-align with the surface for better contact (Fig. 1). Since the adhesive forces of single attachment hairs strongly depended on the contact geometry, our results show that the structures and mechanical properties of the attachment hairs are highly tuned in detail for their specific function of proper contact formation. We anticipate our study to potentially contribute to the development of optimized artificial dry adhesives.

Preliminary reference

Flenner S*, Schaber CF*, Krasnov I, Stieglitz H, Rosenthal M, Burghammer M, Gorb SN, Müller M, 2020. Hierarchical architecture of spider attachment setae reconstructed from scanning nanofocus X-ray diffraction data.

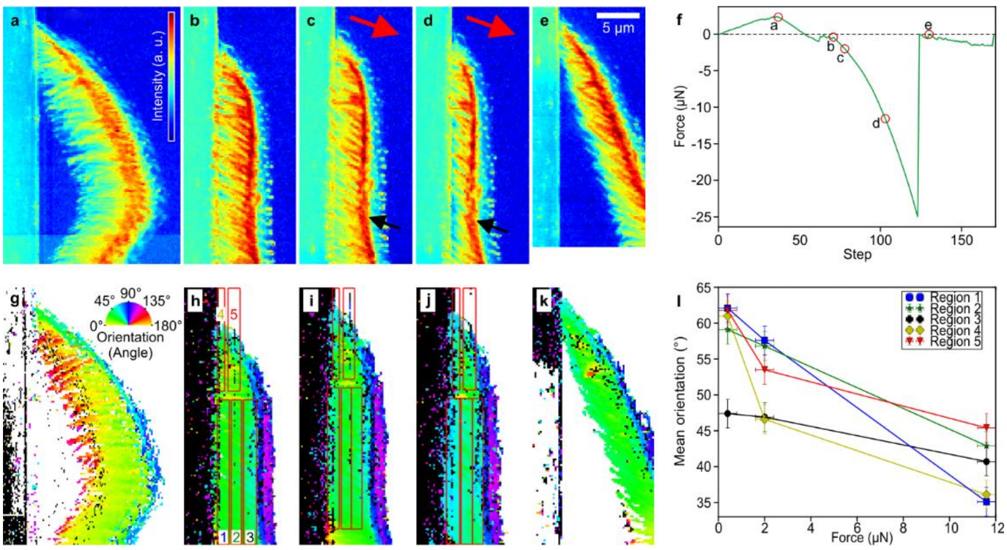

Fig. 1 | Side view of force-controlled attachment and detachment of an attachment hair. **a-e,** SAXS intensity in different states of attachment. **a**, tip attached, **b**, hair fully attached, **c**, pulled, **d**, further pulled, **e**, slipped, but still attached. The direction of the pulling force is indicated by the large red arrows in **c** and **d**. Note the bending of the backbone marked by the black arrows in **b-d**. **f**, Force measured during attachment process. The red circles correspond to the images shown in **a-e** and **g-k**. **g-k**, Orientation maps of the structures corresponding to **a-e**. The red boxes in **h-j** indicate the five regions for which the mean of orientation, shown in **l**, was calculated. **l**, Mean orientation (± standard deviation) in the five different regions marked in **h-j**. In regions 1-3 the orientation changed linearly with different slopes. The maximum deformation was found next to the surface in regions 1 and 4.